Load alleviation in tilt rotor aircraft through active control; modelling and control concepts

B. Manimala, G. D. Padfield and D. Walker
Department of Engineering
University of Liverpool, UK

M. Naddei, L. Verde and U. Ciniglio
Flight Systems Department, CIRA, Italy

P. Rollet and F. Sandri
Eurocopter,
Marignane, France

ABSTRACT

This paper presents the first results from research into active control of structural load alleviation (SLA) for tiltrotor aircraft carried out in the European 'critical technology' RHILP project. The importance of and the need for SLA in tiltrotors are discussed, drawing on previous US experience reported in the open literature. The paper addresses the modelling aspects in some detail; hence forming the foundation for both the FLIGHTLAB simulated XV-15 and EUROTILT configurations. The primary focus of attention is the suppression of in-plane rotor yoke loads for pitch manoeuvres in airplane mode; without suppression these loads would result in a very high level of fatigue damage. Multi-variable control law design methods are used to develop controller schemes and load suppression of 80-90% is demonstrated using rotor cyclic control, albeit at a 20-30% performance penalty. However, rotor flapping transients tend to increase by the action of the SLA system. A dual-objective control design approach demonstrates the effectiveness of suppressing both loads and flapping simultaneously.

NOMENCLATURE

a_1, a_2	left and right rotor gimbal longitudinal tilt
$\dot{a}_1$, $\dot{a}_2$	left and right rotor gimbal longitudinal tilt rates
a_n	normal acceleration
I_β	flap moment of inertia of a rotor blade
M_z	in-plane moment
$M_{zb,1,2,3}$	in-plane moment at the blade root
M_{zpk}	peak in-plane moment
n_x, n_z	longitudinal and normal load factors
P_0, P_1	constants in the In-plane load equation
q	aircraft pitch rate
Q_γ	flight path quickness
Q_l	load quickness
Q_θ	pitch attitude quickness
X_b	pilot longitudinal stick input
η	elevator deflection
η_{sla}	elevator command from the SLA system
γ	flight path angle
Δ_γ	change in flight path angle
Ω	rotor speed
θ_{1s}	longitudinal cyclic pitch at rotor
ψ	blade azimuth

μ-synthesis terms

u_{unc}	input to the actuator
W_d	frequency weight function on the pilot input
W_c	frequency weight function on the performance (in-plane moment output)
$W_{act1,2}$	frequency weights on the actuator performance
W_{inc1}	frequency weights on the input uncertainty
W_{noise}	frequency weight for the white noise on the measurements

Paper No. 2859. Manuscript received 2 October 2003, accepted 23 January 2004.

https://doi.org/10.1017/S0001924000000087 Published online by Cambridge University Press

H-infinity terms

W_Δ	input uncertainty weight
W_{perf}	performance weight
W_u	control weight
W_n	noise weight
z_u	control output
z_{perf}	performance output

1.0 INTRODUCTION

Civil tilt rotor aircraft (CTR) offer promising solutions to rapid short-medium range transport and to congestion relief at busy airport hubs. A large body of opinion reflects this positive view and a significant number of papers over the years have carefully explored and unravelled the technical challenges of these unique hybrids. From the developing understanding it is possible to identify the issues relating to flight dynamics and handling qualities that need special attention in the design of the airframe and associated active flight control system of tilt rotor aircraft. Firstly, while in many ways the flight characteristics and handling qualities of tilt rotor aircraft are conventional in helicopter and aeroplane modes, their behaviour during conversion, and while manoeuvring in the conversion corridor, is less well understood. Secondly, at low speed, manoeuvring close to the ground, the strong aerodynamic inter-actions between the rotor wakes, the airframe and the ground surface can give rise to attitude disturbances and flight path upsets exacerbated by the high disc loading rotors. Thirdly, during flight at steep descent angles, the risk of power settling and vortex ring entry can extend over a larger envelope than for conventional helicopters, also due to the higher rotor disc loadings typical of tilt rotor aircraft, requiring novel technical solutions to envelope protection. Fourth, the large prop-rotors typically found on tilt rotor aircraft are normally gimballed in the hub and manoeuvres in aeroplane or conversion mode can lead to large transient flapping and oscillatory in-plane loads. The resolution of design problems arising from these technical challenges is powerfully aided by accurate modelling and simulation predictions, tailored handling qualities criteria and innovative design concepts, particularly relating to the rotor system and the active flight control system.

This paper is concerned with the fourth issue described above and reports progress on the active control of structural load alleviation in a European civil tilt rotor risk analysis project (RHILP)[1].

Progress in tilt rotor aircraft technology has been led by the US over several decades, and the four technical issues raised above have received due attention and have been reported in the literature. The structural load alleviation (SLA) problem was squarely addressed in the design of the Bell-Boeing V-22 as reported in a series of papers[2-6]. A number of critical loads were identified and active and passive control solutions explored. The present paper will briefly review this work before reporting on analysis and results from the Fifth Framework, European Commission funded, 'critical technology project' — rotorcraft handling, interactions and loads prediction (RHILP) (project co-ordinator Eurocopter). Critical technology programmes are intended to develop sufficient understanding of the critical issues and to develop viable candidate solutions that reduce technical risks to a low enough level for full scale design and development to proceed. Refs 7 and 8 have already reported progress on the conversion handling qualities and aerodynamic inter-action issues addressed in RHILP. The present paper discusses the motivation for active SLA before describing the modelling, control law design and simulation activities. Design work has been conducted on both a 'baseline' XV-15 and Eurocopter's EUROTILT aircraft configurations. In the paper, only results for EUROTILT are presented.

Table 1
Identified critical loads and manoeuvres for the Bell-Boeing V-22[2]

Mode	nacelle angle	Worst case condition	Potential load exceedance
Helicopter and conversion modes	97·5 - 60	Conversion corridor extremes with forward CG	Elastomeric flapping bearing loads
	97·5 - 75	High speed pull-ups	Oscillatory yoke chord bending
	97·5 - 60	Rolling pullouts	Rotor hub flapping
Aeroplane mode	0	High roll rate manoeuvres	Driveshaft & rotor mast torque
	0	Rapid roll reversals	Vertical down-stop & conversion actuator loads
	0	Aggressive pull-ups	Oscillatory yoke chord bending

2.0 MOTIVATION FOR STRUCTURAL LOAD ALLEVIATION

The need for SLA was reported during the design and development of the Bell-Boeing V-22 Osprey. This tiltrotor operates over a broad flight envelope with a manoeuvre capability of up to 4g and speeds up to 345kt. Such a manoeuvre envelope is quite untypical of a conventional helicopter of course. It had been shown through simulation that the loads acting on some the structural components during certain critical manoeuvres resulted in high fatigue usage and, in some cases, exceedence of the design limit. To minimise the manoeuvre loads in the rotor/drive system and the fuselage, structural load limiting laws were incorporated into the active flight control system. The control laws were developed to limit the loads while maintaining Level 1 handling qualities and to not unduly penalise the aircraft manoeuvre capability. Table 1, from Ref. 2, summarises the critical loads for this aircraft. In the present study special attention has been given to the oscillatory yoke chord bending.

2.1 Rotor oscillatory yoke chord bending loads

These loads can occur in high rotor inflow conditions such as high speed flight in aeroplane mode, but also conversion mode. During pull-up and pushover manoeuvres in aeroplane mode, the short period mode is excited, typically resulting in a large pitch rate overshoot, before the steady state manoeuvre is reached. The short period mode is also characterised by significant changes in body axis vertical velocity (aircraft incidence) and perturbations in the rotor plane, effectively acting as longitudinal cyclic inputs, causing the rotor blades to flap in the direction of the aircraft pitch change. The applied aerodynamic moment is then greater than that required to precess the gimballed rotor, leading to an increased flapping in the direction of motion (Fig. 1). The total angular rate of the rotor blades is the sum of the fuselage pitch rate and the gimbal longitudinal flapping rate. This creates a large out of plane aerodynamic moment acting on the rotor. For gimballed rotors it can be shown[5] that one-per-rev. rotor yoke in-plane, or chordwise, bending moments are directly related to the out-of-plane (flap) moments on the rotor. Thus the in-plane bending loads on a tiltrotor in a pull-up manoeuvre are significant and limit the manoeuvrability of the aircraft. Ref. 2 reports that the endurance limit

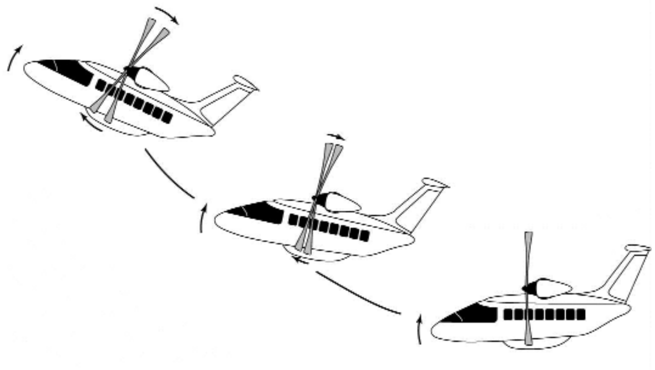

Figure 1. Gimbal flap during pitch-up manoeuvre.

Figure 3. XV-15 in aeroplane mode.

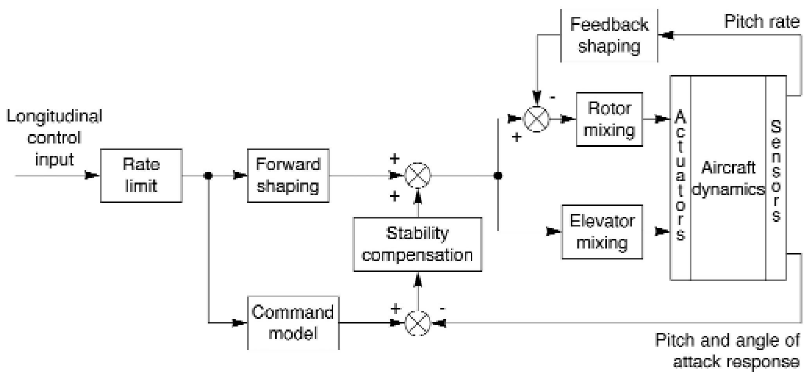

Figure 2. V-22 yoke chord bending load limiter (based on Ref. 2).

of the rotor yoke is reached with a combined pitch rate of slightly less than 25 deg/s at an airspeed of 300kt on the V-22 (i.e. load factor > 6).

The two primary functions of the control laws incorporated in the V-22 flight control system to alleviate the in-plane bending are illustrated in Fig 2 and listed below[2]:

1. reduction of control sensitivity and increase of closed loop system damping: accomplished by transforming the automatic flight control system (AFCS) pitch attitude command model into an angle of attack command model,
2. peak transient body pitch rate and rotor flapping reduced by rate limiting longitudinal stick,

In addition, it was postulated that rotor longitudinal cyclic pitch could be used to cancel the angle-of-attack changes at the rotor caused by aircraft angle of attack, thereby allowing the rotor to precess at the same rate as the nacelle[5]. It is not known whether this additional control function has been incorporated into the V-22. Reference 2 reported results from piloted simulation tests with the SLA system showing a 50% reduction in yoke chord bending and maintenance of Level 1 handling qualities during worst case manoeuvres. Similar performance improvements had been predicted using a combined elevator-cyclic pitch controller designed using eigenstructure-assignment techniques in Ref. 5.

The present paper examines in-plane bending alleviation and continues with a description of the modelling issues.

2.2 Modelling tilt rotor aircraft and critical rotor loads

Within the RHILP project the SLA work package was led by the University of Liverpool with partners CIRA, Eurocopter and Eurocopter Deutschland. The goal was to develop a broad understanding of the specific requirements for load alleviation in Tiltrotor aircraft and to design and test (in simulation) candidate solutions. Successful SLA solutions would be initially tested within the FLIGHTLAB simulation environment at Liverpool before being transferred to the HOST environment[8] and demonstrated to function successfully in Eurocopter's SPHERE simulation facility. Initial exploratory designs would be carried out on the FLIGHTLAB XV-15 (Figs 3 and 4) before being applied to the reference configuration used in RHILP — Eurocopter's EUROTILT (Figs 5 and 6), a design concept derived from the EUROFAR configuration[9,10], sized for 19 pax, 11 tonnes and a range of 600nm.

Within the Flight Science and Technology Research Group at Liverpool, aircraft dynamic models are constructed in the FLIGHTLAB environment[11]. To aid the generation and analysis of flight models, three FLIGHTLAB graphical user interfaces (GUIs) are available: GSCOPE, FLIGHTLAB Model Editor (FLME) and Xanalysis. A schematic representation of the desired model can be generated using the GSCOPE component-level editor. Components are selected from a menu of icons, which are then interconnected to produce the desired architecture and data is assigned to the component fields. When the representation is complete, the user selects the script generation option and a simulation script in FLIGHTLAB's Scope interpretive language is automatically generated from the schematic.

FLME is a subsystem model editor for developing models from higher level primitives such as rotors and airframes. Typically a user will select and configure the subsystem of interest by inputting data values and selecting options that determine the level of fidelity. Models are created hierarchically, with a complete vehicle model consisting of lower level subsystem models, which in turn are collections of primitive components. Hence a model editor tree is constructed, which puts all the predefined aircraft subsystems into a logical 'tree' structure.

The complete model is then analysed using Xanalysis. This GUI has a number of tools allowing a user to change model parameters and examine the dynamic response, stability, performance and handling qualities characteristics of design alternatives.

https://doi.org/10.1017/S0001924000000087 Published online by Cambridge University Press

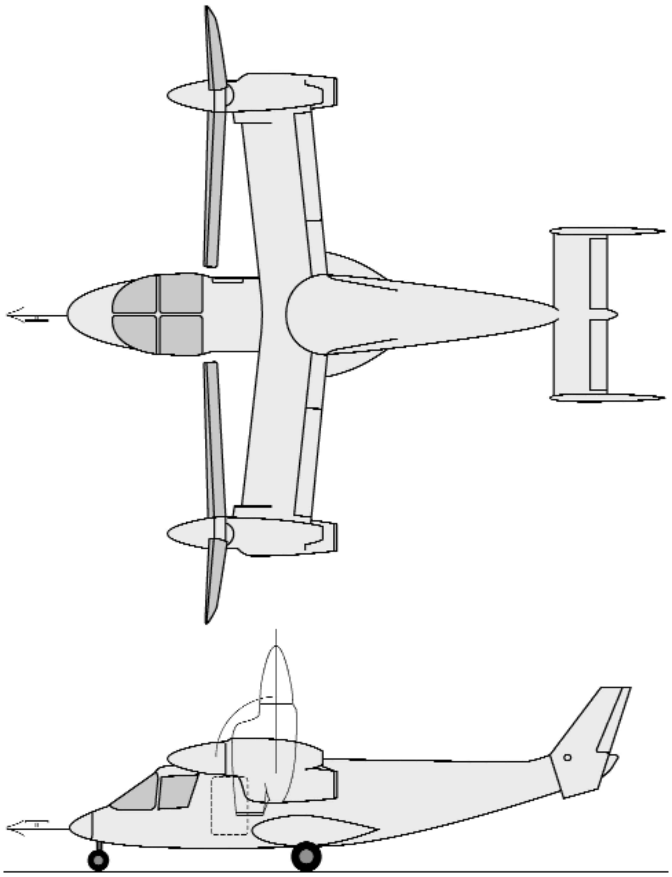

Figure 4. Two-view of XV-15.

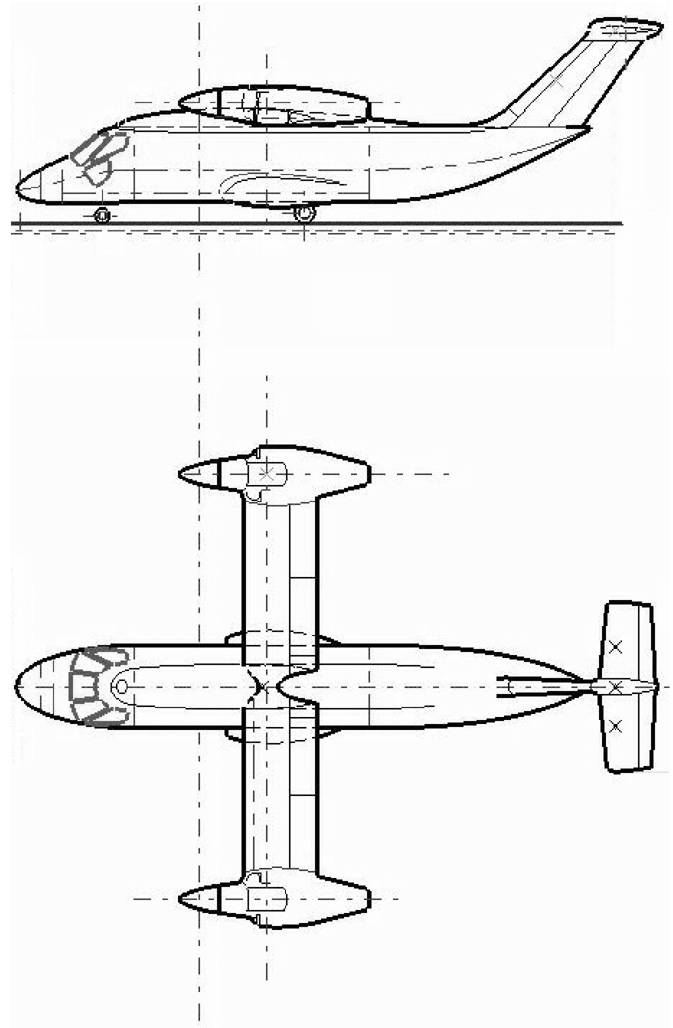

Figure 6. Two-view of EUROTILT.

Figure 5. Artist's impression of EUROTILT.

3.0 FLIGHTLAB XV-15 AND EUROTILT MODELS

As part of the activities of the structural load alleviation work package, Liverpool have developed a FLIGHTLAB model of the Bell XV-15 aircraft based on published data(12-14); this model is designated the FXV-15. The published test data on this aircraft, albeit limited, were used for validation and to generally build confidence in the modelling and simulation activity, before the transfer of the modelling activities to the EUROTILT configuration.

FLIGHTLAB offers several modelling options for the rotor including blade element and Bailey rotor formulations. The rotor hub and the blade retention structure may be modelled from a choice of articulated, gimballed, teetering or rigid formulations. The main features of the FXV-15 and the EUROTILT simulation models are described below.

Both aircraft feature gimballed rotor systems. In FLIGHTLAB, the gimbal is modelled by allowing constrained degrees of freedom in the roll and the pitch axes. This is achieved by the use of two torsional spring-damper components allowing two independent rotations in the rotating hub-system; effectively, they model a rotating spherical spring. The drive component is connected before the rotating springs so that when the springs are deflected (gimbal rotates) the angular velocity vector is no longer aligned with the gimbal *z*-axis. In contrast, the homo-kinetic, constant velocity joint, featured on the V-22, requires that the drive component be connected after the gimbal springs eliminating cyclic variation of the rotor angular velocity.

Although an elastic-blade-element option is available in FLIGHTLAB (within the blade element option), the FXV-15 and F-EUROTILT rotor blades are modelled as rigid beams. For aerodynamic load computations, the blades are divided into equi-annulus grid elements for which blade aero-properties are defined along with chord and twist distributions. Within the FLIGHTLAB aero options, the quasi-steady option was selected which models a two dimensional aerodynamic segment with lift, drag and pitching moment defined as non-linear functions of angle of attack and Mach number. The Peters-He three-state induced flow model was selected for both aircraft models[15]. Ground-effect is modelled by introducing an image system of the rotor and its wake and comes into effect whenever $Z/R \leq 3$, where Z is the height above the terrain and R is the rotor radius.

The aerodynamic data for the lift, drag and the pitching moment coefficients of the wing are tabulated against angle of attack, flap setting and the nacelle tilt (Ref. 12 for the XV-15). A new FLIGHTLAB component was created, which calculates the lift, drag and pitching moment in the local wind axis system depending on the current values of angle of attack, flap setting and nacelle angle. The effect of aileron input on the FXV-15 is implemented by calculating the increment in lift on the wing through a control effectiveness coefficient. The wing is treated in four segments. The outer left and right sections are immersed in the rotor slipstream and the two inboard sections are assumed to be out of the rotor wake. The rotor wake impingement on the wing has been implemented for all nacelle angles by superimposing a factored component of the uniform induced velocity onto the vehicle free stream velocity:

For EUROTILT, the wing and the fuselage are modelled as a single aerodynamic super-component which calculates the aerodynamic forces and moments by using multivariable, non-linear polynomial functions of angle-of-attack, side-slip angle, flap setting and aileron angle. These polynomials are derived from a combination of wind tunnel test data and theoretical estimates. Roll and yaw damping due to the wing are also modelled by the use of damping coefficients that are functions of attitude rates.

For the FXV-15, the horizontal stabiliser and the vertical fin are modelled in the same manner as the wing. Look up tables are used to derive the lift and drag coefficients corresponding to the angle of attack and the rudder or elevator setting. For EUROTILT, super components are used, which compute the lift, drag and moment coefficients through polynomial functions.

Based on the data in Ref. 12, the effect of rotor wake on the horizontal stabiliser is modelled by adding an equivalent induced velocity component and applying a flow deflection to the free stream velocity vector at the horizontal stabiliser. The version of FLIGHTLAB EUROTILT used in the structural load alleviation work does not include the specific low-speed interaction effects developed within the companion RHILP work package[8], e.g. rotor/wing interference, fountain flow effects, ground effect of a rotor in proximity of a wing.

Fuselage aerodynamic forces and moments for the FXV-15 are derived from Ref. 12. The EUROTILT fuselage aerodynamics are included in the wing super-component.

The unique engine-governor system of the XV-15 was used as the basis for both aircraft featuring a first order relationship between output and commanded torque; the latter is a function of throttle setting and atmospheric conditions, with throttle and collective geared together as a function of nacelle tilt. The rigid drive train system was modelled as a collection of gear, drive, clutch and bearing components with the interconnect shaft as the single degree of freedom driven by the resultant torque.

The FXV-15 control system features the mechanical interlinks between the pilot's controls and the rotor and fixed-wing control surfaces, with gearings set as functions of nacelle angle. The system also includes three-axis stability and control augmentation, with rate

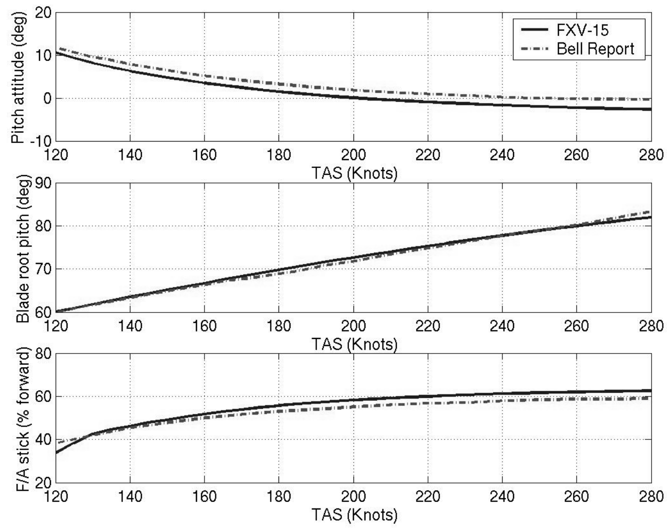

Figure 7. Comparison of FXV-15 and Bell simulation[12] trims (aeroplane mode).

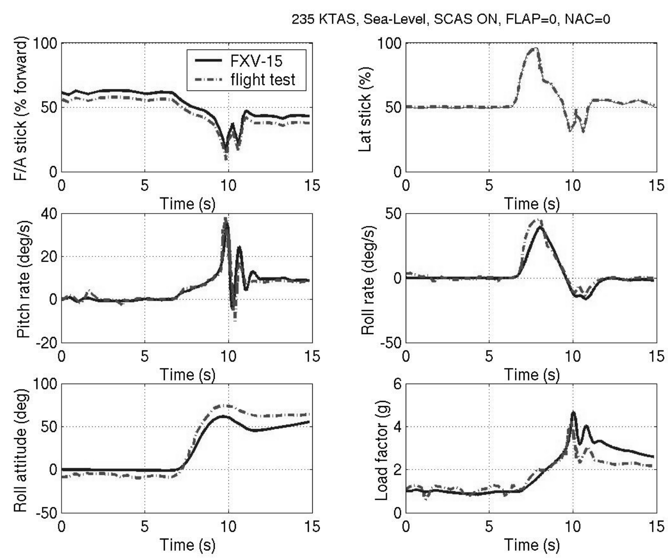

Figure 8. Comparison of FXV-15 with flight test data in a 4g turn, aeroplane mode[13].

damping and feed-forward response quickening. The EUROTILT control mixing structure is similar to the XV-15. The stability augmentation system features rate damping in three axes.

A comparison of FLIGHTLAB results with published XV-15 data are shown in Figs 7-10. Figure 7 compares variations in aircraft pitch angle, collective pitch and fore/aft stick with results from the Bell simulation model[12] in aeroplane mode as a function of airspeed. The FXV-15 trims at a lower pitch angle and further forward stick than the Bell simulation. It is suspected that the latter does not include the built-in wing incidence of 3 deg which would account for the relatively constant offset over the speed range shown. There is very good agreement with the collective root pitch angle.

Figure 8 shows a comparison of FXV-15 results with flight test data for the case of a 4g turn at 235kt[13]. Pitch and roll rate peaks are predicted to within about 10% giving confidence in modelling of the basic flight mechanics.

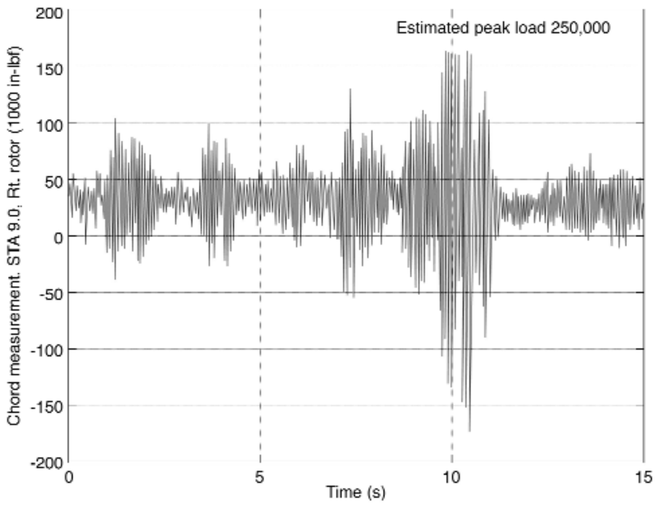

Figure 9. Yoke chord moment during 4g turn — flight test (based on Ref. 13).

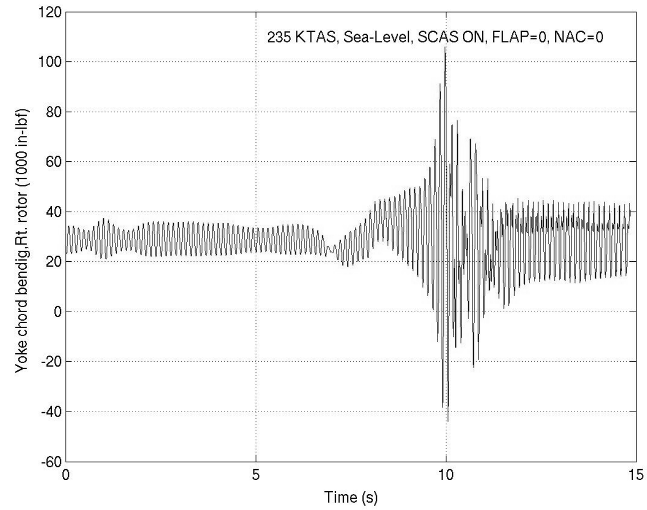

Figure 10. Yoke chord moment during 4g turn — FXV-15.

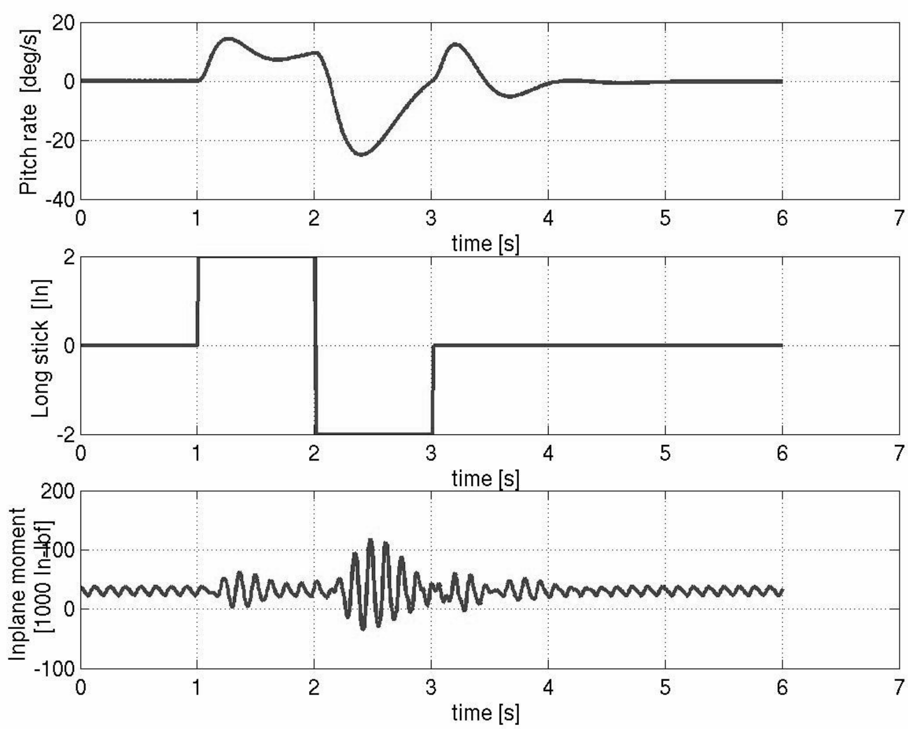

Figure 11. Yoke bending and pitch rate XV-15, 2.5g pull up, 250kt.

Finally, Figs 9 and 10 compare the yoke chord bending moment on the right rotor during the 4g turn shown in Fig 8. The flight data shows a slightly higher level of mean trim moment (rotor torque — 35,000 cf 30,000in-lb) and much larger excursions during the manoeuvre (140,000 cf 80,000in-lb). Satisfactory explanations for these differences have not been found, but the in-plane loads are closely related to the gimbal flap response and are dominated by the lift forces and strongly affected by 3D aerodynamics on the tips of the highly twisted blades with their rotating wake; these effects are notoriously difficult to predict with accuracy.

The comparisons call for deeper analysis of the modelling but for the present purposes, the FLIGHTLAB response levels were considered adequate for preliminary SLA investigations. In this context Ref. 2 discusses the simulation model enhancements required to model the V-22 yoke bending through empirical corrections derived from flight test data and an advanced aeroelastic rotor model.

4.0 ANALYTIC APPROXIMATIONS TO THE YOKE CHORD BENDING FOR CONTROL SYNTHESIS

Figure 11 shows the pitch rate, longitudinal control and in-plane bending at the blade yoke for the FXV-15 in a 2·5g pull-up manoeuvre at 250kt. It can be seen that the peak loads correlate closely with the pitch rate peaks.

Miller and Ham[5] showed that the most significant term in the in-plane moment expressions is given by the aerodynamic moment balancing the gyroscopic moment acting on the gimbal, M_{gyro}:

$$M_{gyro} = 2I_\beta\Omega\,(q + \dot{a}\,)\mathrm{Sin}(\psi) \qquad \ldots (1)$$

https://doi.org/10.1017/S0001924000000087 Published online by Cambridge University Press

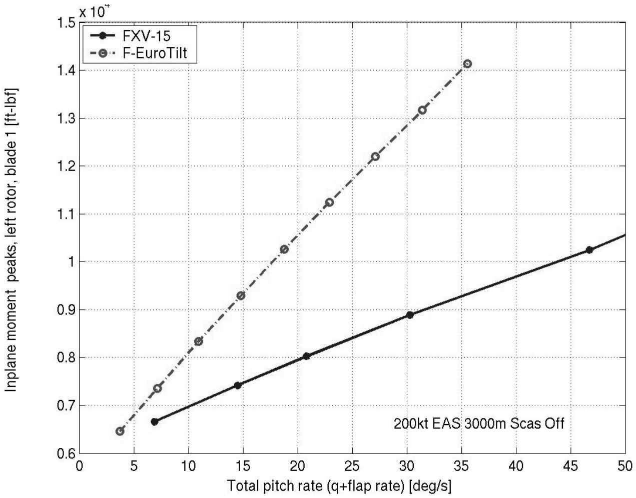

Figure 12. Correlation of peak in-plane load with total rotor pitch rate.

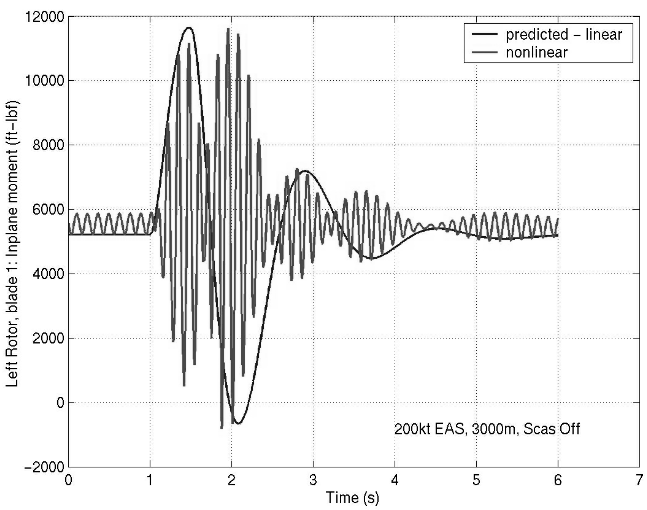

Figure 13. In-plane bending moment in a 2·5g pull-up manoeuvre (200kt, 3,000m): FXV-15.

where I_β is the flapping moment of inertia of a rotor blade, Ω is the rotorspeed and $\dot{a}$ and q are the gimbal longitudinal flap rate and pitch rate respectively.

As noted earlier, the body axis vertical velocity induced by a pull-up manoeuvre causes the rotor disc to flap in the same direction of the aircraft pitch rate, giving rise to large in-plane loads. It can be shown that the magnitude of the in-plane moment is approximately proportional to the total pitch rate (aircraft pitch rate + gimbal rate). Figure 12 shows a fairly linear correlation between the peak in-plane load and the total angular rate for the case of 200kt equivalent airspeed (EAS) at 3,000m altitude. We have shown here a comparison of results for the FXV-15 and EUROTILT with stability and control augmentation disengaged. The range of total gimbal pitch rate has been deliberately exaggerated (compared with the manoeuvre envelope of a civil tilt rotor) to highlight the linearity for large amplitude manoeuvres.

For the development of SLA controllers it is necessary to develop linear output equations relating the controlled variable (in-plane bending) with available measurements. Based on the above arguments, output equations relating the total pitch rate and the envelope of the in-plane loads were derived in the form;

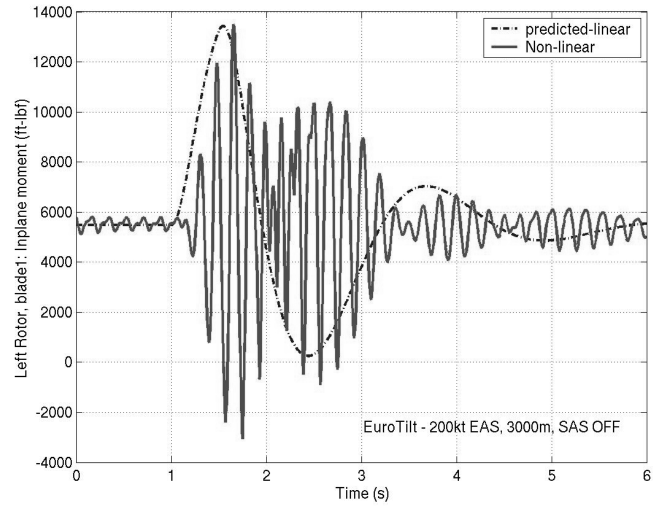

Figure 14. In-plane bending moment in a 2·5g pull-up manoeuvre (200kts, 3,000m): EUROTILT.

$$M_z = q_{tot}P_1 + P_0 \qquad \ldots (2)$$

where q_{tot} is the total gimbal pitch rate.
$q_{tot} = q - \dot{a}_2$, for the left rotor (clock-wise)
$q_{tot} = q + \dot{a}_2$, for the right rotor (counter-clockwise)

In FLIGHTLAB, a gimbal deflection in the aircraft 'nose-up' direction (positive pitch rate) is positive for the right rotor and negative for the left rotor.

Comparisons of the FXV-15 and EUROTILT non-linear chord bending response with the linear estimations using Equation (2) for a nominal 2·5g pull-up manoeuvre are given in Figs 13 and 14. They show good agreement between estimated values and the non-linear simulation.

Initially attempts were made to extract linear output equations for the in-plane loads from the non-linear FLIGHTLAB model through numerical differencing of the non-linear output function representing the in-plane loads. This procedure led to inaccurate predictions due to the periodic nature of the individual blade hub moments. Hence a new approach, making use of a multi-blade co-ordinate (MBC) transformation[16] to transform the in-plane loads from the individual blade co-ordinates to a hub fixed co-ordinate frame was used. In multi-blade coordinates the loads have a period of 3/rev on both aircraft types, but many of these combined effects cancel out. A dominant effect is the quasi-steady 0/rev envelope during manoeuvres.

The individual blade in-plane loads $M_{zb,1}$, M_{zb2} and M_{zb3}, at the root of each of the three blades are transformed into a load envelope in multi-blade co-ordinates using the transformation.

$$\begin{bmatrix} M_{z_0} \\ M_{z_c} \\ M_{z_s} \end{bmatrix} = 1/3 \begin{bmatrix} 1 & 1 & 1 \\ 2\text{Cos}(\psi_1) & 2\text{Cos}(\psi_2) & 2\text{Cos}(\psi_3) \\ 2\text{Sin}(\psi_1) & 2\text{Sin}(\psi_2) & 2\text{Sin}(\psi_3) \end{bmatrix} \begin{bmatrix} M_{z_{b1}} \\ M_{z_{b2}} \\ M_{z_{b3}} \end{bmatrix} \qquad \ldots (3)$$

where the azimuth angle for the ith blade,

$$\psi_i = \Omega t + (i - 1)\, 2\pi/3 \qquad \ldots (4)$$

The envelope of the load is then defined as the sum of the three first harmonic terms;

$$M_z = M_{z0} + M_{zc} + M_{zs} \qquad \ldots (5)$$

https://doi.org/10.1017/S0001924000000087 Published online by Cambridge University Press

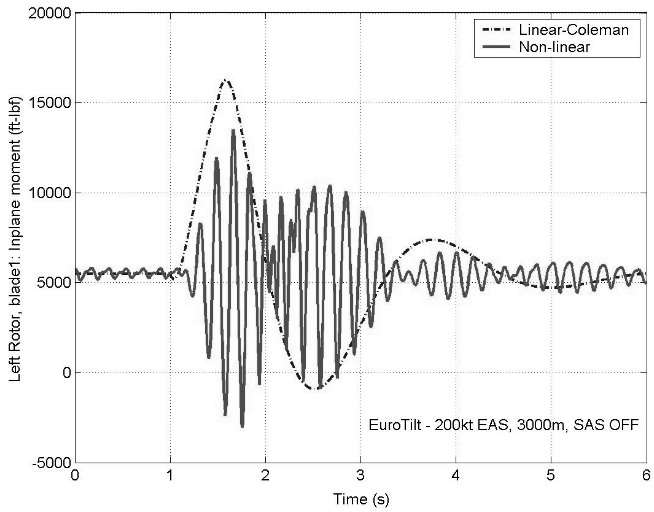

Figure 15. In-plane moment blade root for a 2·5g pull-up manoeuvre; EUROTILT.

Figure 15 presents a comparison of the MBC load envelope with the nonlinear blade load and linearised approximation for EUROTILT in the 2·5g manoeuvre.

There is a reasonable agreement between the linear and non-linear load envelopes, thus giving the control system designer an option of minimizing the predicted output equation or the linearised output equation expressed in terms of the total pitch rate.

5.0 LOAD ALLEVIATION CONTROL CONCEPTS

In this section the structure of the SLA controller is discussed, together with the design concepts applied to the EUROTILT configuration. As already described, the problem of prop-rotor SLA in aggressive pull-up manoeuvres was addressed in the design of the automatic flight control system (AFCS) of the Bell-Boeing V-22 Osprey aircraft (see also Ref. 17). The oscillatory yoke chord bending load limiter on this aircraft features modifications to the AFCS command model/stability compensation and rate limitation of the longitudinal stick command.

The SLA controller described in Refs 4 and 5 used a modified Eigen-structure assignment technique. The controller described in Ref. 5 utilised feedback of pitch rate, pitch angle and normal velocity to generate control inputs on rotor cyclic pitch angles. As an observation, the study shows that the use of rotor flapping states in the feedback is not necessary for suppression of the in-plane loads. Stability robustness of the controller is demonstrated by means of singular value analysis where high frequency modelling errors are represented as a multiplicative error at the system input.

Two different approaches to the development of control laws for rotor yoke chord load alleviation are investigated in Ref. 4. The first controller used flapping feedback to regulate longitudinal and lateral cyclic pitch angles. Note that the V-22 is equipped with triple redundant flapping transducers; a rotor trimming function is incorporated in the primary flight control system to limit steady-state rotor flapping in forward flight[4]. As the compensator did not meet the stability robustness requirements, a second control system was developed using eigen-structure assignment methodology. The resulting pitch rate feedback control law, utilising longitudinal cyclic pitch and elevator, provided a favourable match between the desired and achieved short period Eigen-structure and was robust to structural mode parameter uncertainties.

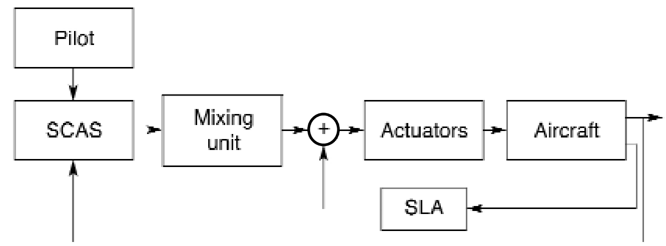

Figure 16. Basic SLA controller structure (μ-synthesis).

The paper continues with the design activity in the present study aimed at the suppression of in-plane loads during manoeuvres in aeroplane mode using robust multivariable control theory. The RHILP project has investigated SLA controllers for both the XV-15 and EUROTILT aircraft. Only results for EUROTILT are presented here. Both μ-synthesis and *H*-infinity techniques were explored in parallel, independent studies and a selection of results from each will be presented.

5.1 μ-synthesis spproach

μ-synthesis is a frequency domain synthesis technique that allows the designer to take into account external disturbances, model uncertainties and to assign an ideal model based on HQ requirements.

Each of these elements can be characterised in the frequency domain by means of a suitable weighting function W. The synthesis scheme is called interconnection structure and has several input and output channels, where all the input and output signals are assumed to be between –1 and 1. The reader is referred to Refs 18 and 19 for more detail. The basic structure of the SLA control system is given in Fig. 16.

The controller sees the pilot command (i.e. longitudinal stick displacement) as a ‘disturbance’ that produces yoke chord bending moments. The SLA system then operates to alleviate this phenomenon, with minimal modification to the vehicle flight dynamics. The SLA system uses some of the aircraft motion states as input, and acts at the exit of the mixing unit (Fig 16). Located in the inner loop, it therefore impacts the flight dynamics and therefore the HQs provided by the SCAS, as the total command to the actuators is the sum of the SLA output and the SCAS command. In the initial design exercises, the controller is synthesised iteratively until acceptable handling qualities were obtained. In the following, only results for the rotor cyclic control of in-plane loads are presented.

5.2 Performance and handling qualities evaluation

In RHILP it was proposed that the flight path quickness should be adopted as the criterion for quantifying the SLA system effect on handling qualities (HQs), during pitch manoeuvres in aeroplane mode. Quickness is a hybrid measure of how quickly a manoeuvre can be performed[20]. Specifically, it is defined as the ratio of peak rate of change of motion to the motion change, when considering the response to a singlet command (for rate command response type).

For a singlet input in longitudinal control, pitch rate and flight path angle rise to their maximum values following the first step command and, after the second step on the control input, new steady state values of flight path angle and pitch attitude are obtained. With γ the flight path angle and Δγ the change in flight path, the flight path quickness Q_γ is written as;

$$Q_\gamma = \frac{\dot{\gamma}_{pk}}{\Delta\gamma} \qquad \text{. . . (6)}$$

https://doi.org/10.1017/S0001924000000087 Published online by Cambridge University Press

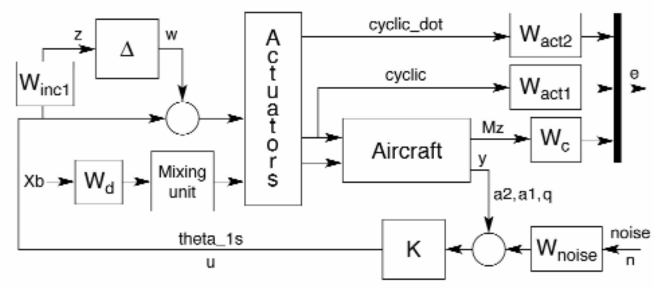

Figure 17. μ-synthesis scheme.

Assuming the forward velocity remains constant at the trim or equilibrium value U_e, the flight path quickness can be written as,

$$Q_\gamma = \frac{g\,(n_{zpk} - 1)}{U_e \Delta\gamma} \qquad \ldots (7)$$

where n_z is the normal load factor defined as

$$n_z = -a_n/g + 1 \qquad \ldots (8)$$

and a_n is the normal acceleration.

It can be shown[20] that in the limiting cases, the flight path quickness can be written as,

$$\begin{aligned} &Q_\gamma \Rightarrow -Z_w \quad && \text{as } \Delta\gamma \Rightarrow 0 \\ &Q_\gamma \Rightarrow Q_\theta \quad && \text{as } \Delta\gamma \Rightarrow \infty \quad \left(Q_\theta = \frac{q_{pk}}{\Delta\theta} \right) \end{aligned} \qquad \ldots (9)$$

where Z_w is the heave damping derivative.

A complementary load metric, namely the load quickness, can be derived in a similar way. For the rotor yoke in-plane moment, we take the time history of the peak of the one/rev in-plane load component M_z and define the load quickness,

$$Q_l = \frac{M_{z\,pk}}{\Delta\gamma} \qquad \ldots (10)$$

These two parameters provide consistent measures in the evaluation of load suppression and HQ effects. To the same end, frequency responses of flight path angle and pitch rate with SLA-on *vs* SLA-off are also investigated in this study.

5.3 Design scheme

The expanded control structure used in the synthesis of the SLA system is shown in Fig. 17.

The following hypotheses were used in the control system design methodology:

1. Gimbal flap dynamics are included but in-plane motion is restricted to rotorspeed variations; a 12-state linear system model was used for control synthesis;
2. Rotor and elevator actuator bandwidths are 60 rad/s;
3. Longitudinal cyclic slew rate is 30 deg/s;
4. Reference flight condition: 200 knots EAS (3,000m),
5. Off-nominal flight conditions for the evaluation of robustness: 160 knots EAS, sea level and 225 knots EAS, 6,000m,
6. Longitudinal pulse manoeuvre (0·5s singlet) is used for the evaluation of the SLA performance.
7. Uncertainty on actuator gain: ±40%, a somewhat arbitrary value intended to present a demanding test for the design.

Based on the above assumptions, the following weight functions (see Fig. 17) are chosen:

$$W_d = \frac{2 \cdot 25}{1 + s/10} \qquad \ldots (11)$$

$$W_c = \frac{1}{C(1 + s/10)} \qquad \ldots (12)$$

$$W_{noise} = 10^{-4} \qquad \ldots (13)$$

$$W_{incl} = 0 \cdot 4 \qquad \ldots (14)$$

$$W_{act1} = \frac{1}{\mu_p(1 + s/10)} \qquad \ldots (15)$$

$$W_{act2} = \frac{30}{s + 1} \qquad \ldots (16)$$

The parameter C in the W_c weight transfer function has the physical meaning of the maximum allowed steady state moment peak, whereas μ_p in the W_{act1} weight function represents the steady state control authority. The uncertainty of ±40% on actuator gain is realised by means of the W_{incl} function. The input to the actuator, u_{unc}, is given by the control command u multiplied by the transfer function $W_{incl} + \Delta$, i.e.

$$u_{unc} = (W_{incl} + \Delta)\, u \qquad \ldots (17)$$

Therefore, as Δ varies between –1 and 1, (as prescribed when μ-theory is applied), the variation of u_{unc} is in the range $0{\cdot}6u$–$1{\cdot}4u$.

A major goal of the approach is to obtain C as low as possible, with a limited control authority μ_p. In other words we try to obtain a reasonable trade-off between performances and control authority. In the present study, a control authority limitation of 4 deg was set as a requirement for the EUROTILT configuration.

5.4 Selection of measurements and actuator configuration

Following the definition of the so-called uncoupled scheme[19] for controller synthesis, an optimum configuration of sensors and measurements needs to be defined. As a general criterion, no additional actuators or sensors with respect to those already present in the flight control system should be used, and the SLA system should have a minimum impact on HQs.

In the first synthesis, combined (longitudinal) cyclic commands are selected as the only control signal. At the first cut of the design stage, three different sensor configurations were selected, based on control effectiveness and observability considerations:

1. Case 1: a_2, a_1, q (longitudinal gimbal flapping of right and left rotor and pitch rate);
2. Case 2: q (pitch rate only); and
3. Case 3: n_x, n_z, q (longitudinal and vertical load factors and pitch rate).

Different controllers were designed by using the above three measurement configurations and assessed by examination of the transfer functions M_z/X_b and q/X_b, where X_b is the longitudinal control. The following conclusions were drawn.

1. All the three cases resulted in good performance at the reference flight condition.

https://doi.org/10.1017/S0001924000000087 Published online by Cambridge University Press

Table 2
SAS-off parametric analysis

Cyclic range (deg)	**6·5**	**4·1**	**1·2**
M_{zpk} (lb-ft)	905	4,720	9,050
Q_γ (1/sec)	1·93	2·17	2·23

Table 3
SAS-on parametric analysis

Cyclic range (deg)	**3·9 (selected)**	**2·3**	**0·7**
M_{zpk} (lb-ft)	800	2,900	5,350
Q_γ (1/sec)	1·23	1·35	1·44

2. Transfer functions from X_b to a_2 and a_1 are less influenced by flight conditions than those from X_b to n_x, n_z or q (Cases 2 and 3). For this reason, the SLA system obtained with Case 1 can manage a greater degree of variation in system dynamics than the controller designed using load factor components as inputs. Indeed, a typical disadvantage of normal acceleration feedback is that the gain of the elevator-to-normal-acceleration transfer function varies widely with dynamic pressure[21].

A control structure providing consistent performance at varying flight speeds is clearly preferred, hence the synthesis of the controller utilising the two gimbal angles and the pitch rate as feedback measurements is presented in detail. Although the use of gimbal rates (Case 1) was initially disregarded due to the inherent difficulties in their direct measurement, it is interesting to note that rotor tilt angles, a_2 and a_1, are used on the Bell-Boeing V-22 Osprey tilt rotor aircraft[2,4] to limit trim rotor flapping.

5.5 Parametric analysis

In the optimisation of the SLA control system, a parametric analysis was initially carried out. The open-loop response characteristics in terms of yoke chord bending moment and flight path quickness parameter were computed for both stability augmentation system (SAS) on and off, as;

1. M_{zpk} open loop SAS-off = 10,750 [ft-lbf]
2. M_{zpk} open loop SAS-on = 6,300 [ft-lbf]
3. Q_γ open loop SAS-off = 2·3 [1/sec]
4. Q_γ open loop SAS-on = 1·47 [1/sec]

After a number of trial and error iterations, three controllers were obtained where the closed-loop μ function was <1 over the chosen range of frequencies. The results of the synthesis are summarised in Tables 2 and 3 for the 4 deg flight path change manoeuvre. Each column refers to a SLA system with different cyclic control authority.

Figures 18 and 19 show, respectively, the peak values of the in-plane moment, normalised with respect to its maximum value in the open loop case, and the normalised flight path quickness parameter, as functions of maximum displacement of longitudinal cyclic due to controller activity.

The results show that, as expected, performance improves for higher control authority with an associated penalty on the flight path quickness. For example for the SAS-off case, and with a cyclic authority of 4 deg, the 57% reduction in yoke load quickness

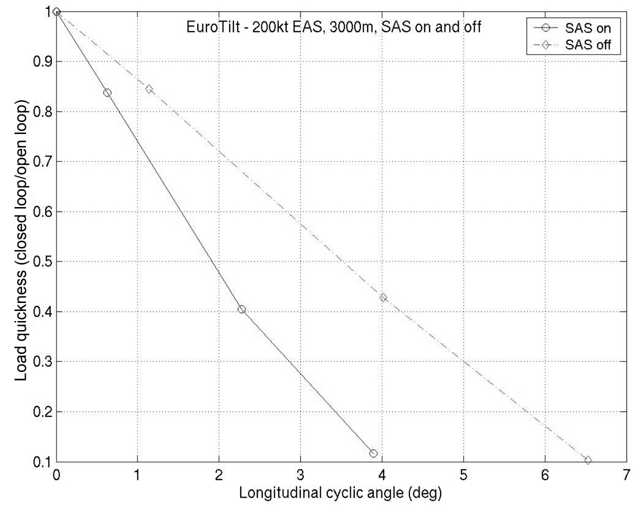

Figure 18. Normalised moment quickness at reference condition.

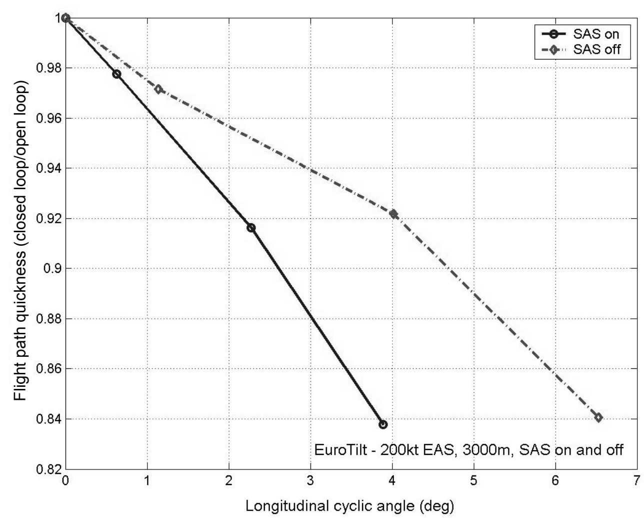

Figure 19. Normalised flight path quickness, reference condition.

is accompanied by a reduction in flight path quickness of about 8%. Full load suppression requires about 7 deg cyclic with SAS-off giving a corresponding HQ degradation of about 20%. One of the design goals was to limit control authority for the SLA system to 4 deg of longitudinal cyclic and hence the 3·9 deg (see Table 3) authority controller case was chosen for further analysis.

5.6 Reduction of controller order

The selected SLA controller had 32 states, a bandwidth of about 4·6 rad/s and a maximum eigenvalue at 495rad/s. In order to reduce the controller order for the purpose of implementation in the nonlinear EUROTILT simulation, a Hankel model reduction procedure[22] was carried out to give a 12 state controller and a further residualisation to 7 states (max Eigenvalue –5·13rads/s), accounting for the low frequency contribution of the truncated modes.

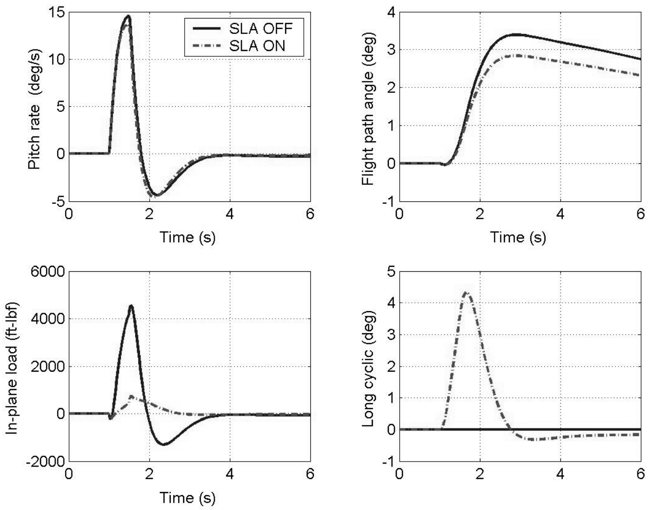

Figure 20. Time domain analysis: EUROTILT, 160kt; SAS ON

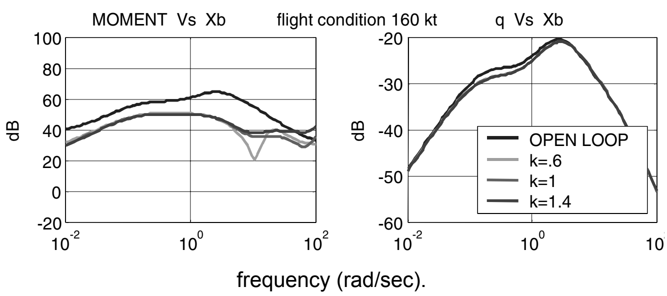

Figure 21. Frequency domain analysis: EUROTILT, 160kt, SAS ON.

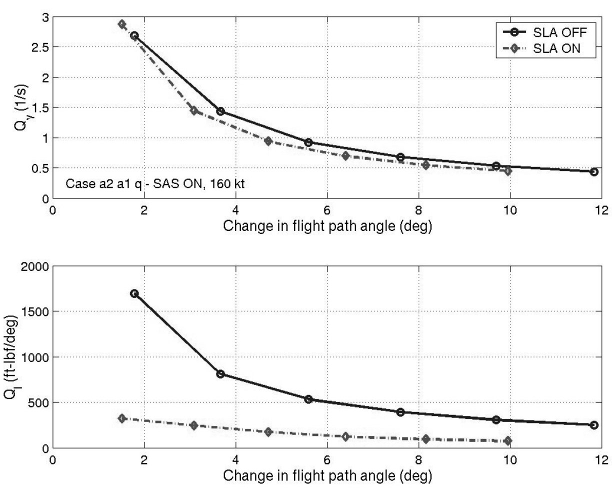

Figure 22. Quickness parameters: EUROTILT, 160kt SAS ON.

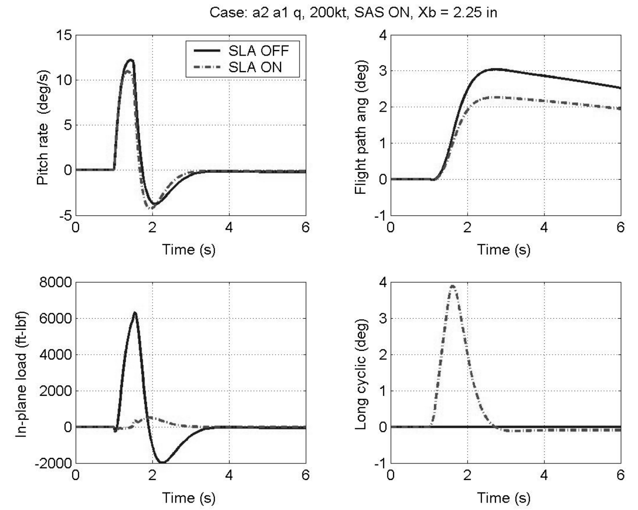

Figure 23. Time domain analysis: EUROTILT, 200kt SAS ON.

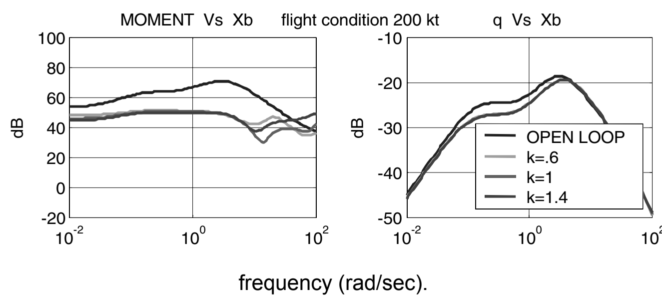

Figure 24. Frequency domain analysis: EUROTILT, 200kt, SAS ON.

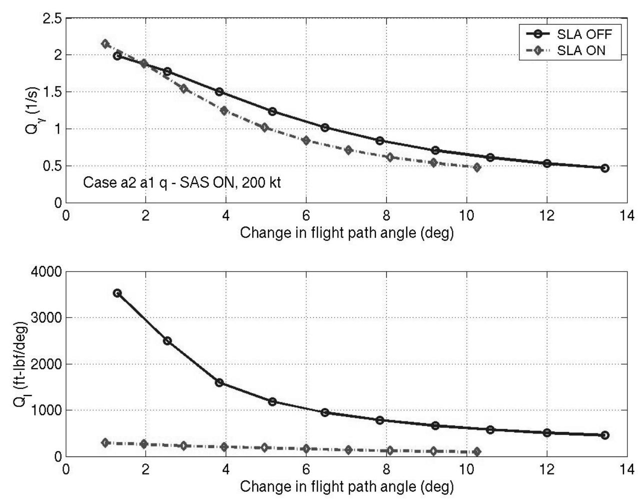

Figure 25. Quickness parameters: EUROTILT, 200kt SAS ON.

5.7 Performance and HQ analysis

The final control system was effective in reducing the in-plane moment at the design and off-design flight conditions. Results for time domain, frequency domain and quickness analysis for all three flight cases are shown in Figs 20-28. The control action was also maintained within the required constraints, i.e. longitudinal cyclic lower than 4 deg. The parameter k in the Bode plots is used to evaluate the effect of output uncertainty on controller performance (i.e. ±40% changes). For the time domain analysis, elevator singlet pulses were applied to achieve approximately 2·4g at all three speeds (0.5 sec duration; three inch at 160kt, 2·25 inch at 200kt and one inch at 225kt; stick travel ±5 inch).

The load suppression is clearly shown in the singlet response time histories. Also, the flight path performance is reduced by approximately 10, 15 and 30% relative to the SLA-off case as speed increases. The Bode amplitude plots show that this suppression is effective over a wide frequency range. In the range 10-20rad/sec, the

https://doi.org/10.1017/S0001924000000087 Published online by Cambridge University Press

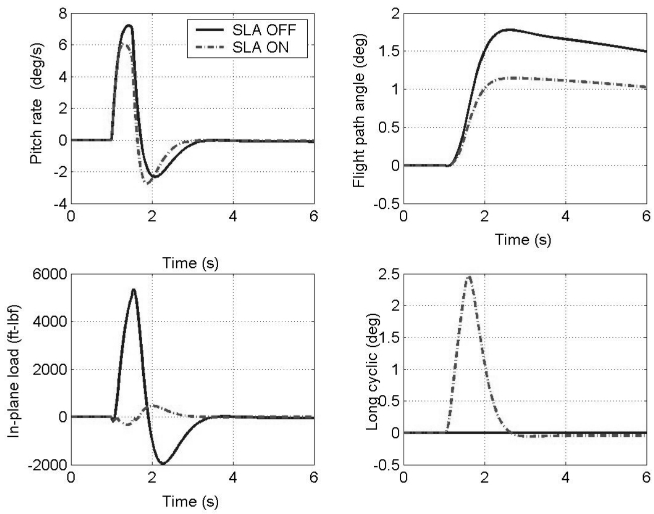

Figure 26. Time domain analysis: EUROTILT, 225kt SAS ON.

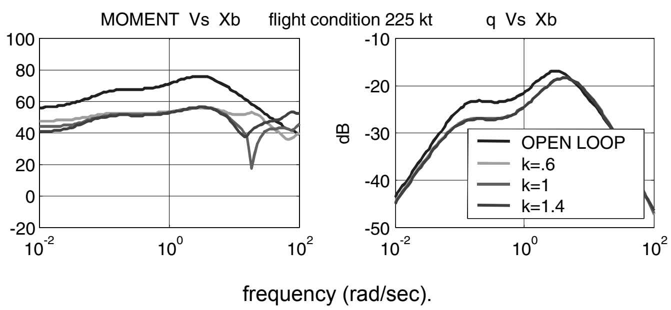

Figure 27. Frequency domain analysis: EUROTILT 225kt, SAS ON.

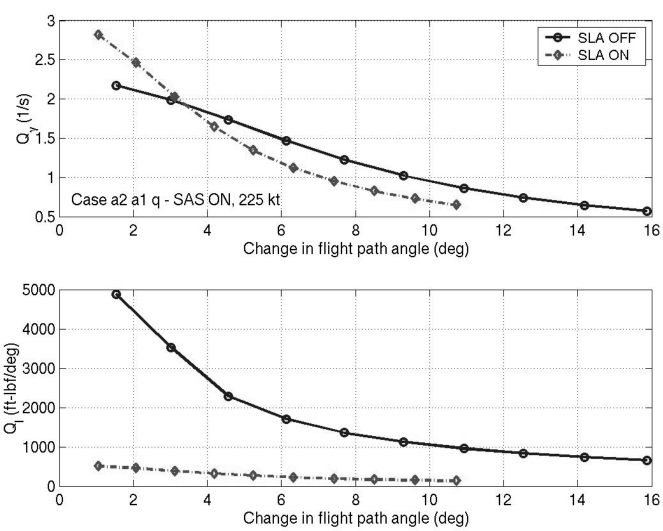

Figure 28. Quickness parameters: EUROTILT, 225kt SAS ON.

uncertainly analysis predicts a sensitivity, related to the choice of weight functions, that warrants further analysis; both increased and reduced actuator gains appear to increase the response by more than 20db. The quickness charts confirm the suppression effects and also show an unexpected improvement in flight path performance for small changes, an effect that also needs further investigation, but is suspected to be related to the increased bandwidth of the pitch rate response with SLA engaged.

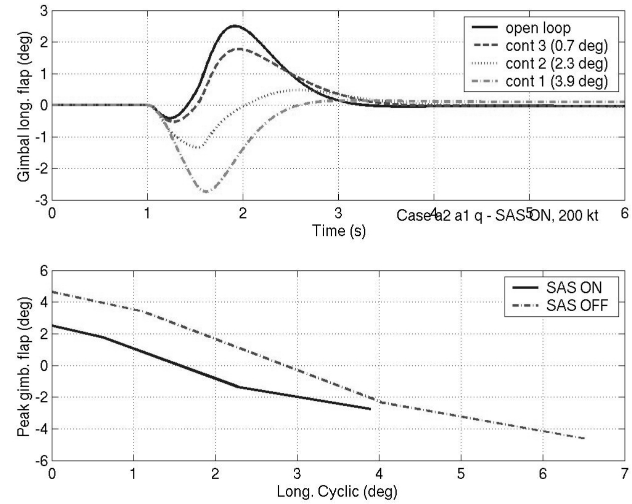

Figure 29. Gimbal flap *vs* longitudinal cyclic authority.

5.8 Rotor flapping

As previously discussed, the fundamental cause for the amplification of the in-plane load during a pull-up manoeuvre is that the rotor longitudinal flap rate and the aircraft pitch rate occur in the same direction. Principally the SLA controller reduces the in plane load by forcing the rotor to flap against the pitch rate through the application of longitudinal cyclic. For this kind of SLA system, it was noted that the magnitude of the longitudinal flapping is directly related to the applied cyclic angle.

These effects are illustrated in Fig. 29 where the gimbal flap time histories and peaks are presented for the reference manoeuvre at 200kt, for the three controllers designed with varying authority; results for SAS on and off are compared. The 4 deg SLA system effectively reverses the gimbal flap. Note the initial tendency for the rotor to flap down (–ve) following the elevator input for the open loop case, before the incidence changes cause the in-plane velocities to grow and precess the rotor ahead of the nacelle. Reducing gimbal flap is also a concern in tilt rotor aircraft and results are presented in the next section from an investigation integrating in-plane bending and flap suppression.

5.9 SLA control law for combined bending moment and gimbal flap reduction

The control law described in the previous section was designed to attenuate in-plane bending moments (M_z) using longitudinal cyclic (θ_{1s}). This it did effectively. However, its use of the cyclic resulted in what were felt to be excessive excursions in gimbal longitudinal flapping. This section describes the work carried out to determine whether, by giving the SLA system authority over elevator as well as over longitudinal cyclic, it would be possible to suppress both the in-plane load and the gimbal longitudinal flap in aeroplane mode, while minimising the negative impact on HQs. This time, *H*-infinity optimization was chosen for the synthesis, partly to reduce the order of the control law.

The configuration adopted is shown in Fig. 30. Pitch-rate (q) and gimbal flap (a_1) are fed back to elevator and longitudinal cyclic via a simple two-input, two-output control law. The net elevator demand is the sum of the raw elevator demand η (which is determined by the pilot and/or the SCAS) and the SLA elevator demand η_{sla}.

The design of the SLA law can now be formulated as a disturbance rejection problem. The disturbance η_{sla} drives the plant dynamics and forces the outputs M_z and a_1 away from their trim

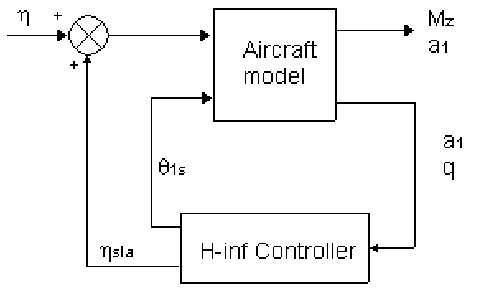

Figure 30. Structure of *H*-infinity SLA control loop.

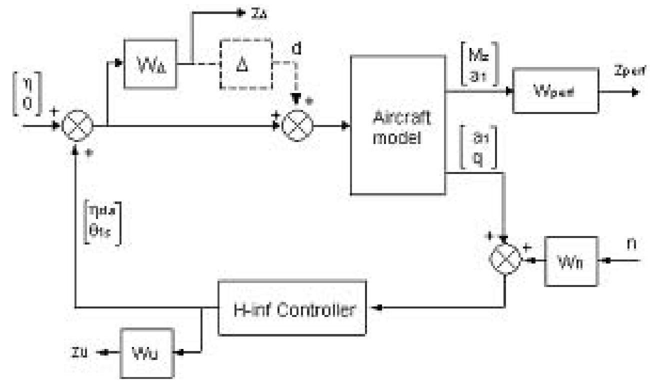

Figure 31. Interconnection structure used for dual-objective SLA design.

values. The objective is to synthesize the control law so as to reduce the closed-loop transmission from η_{sla} to $\{M_z, a_1\}$ using the available measurements and controls.

5.10 Controller design process

The design was based on an eight-state linear model representing the 200kt straight-and-level reference condition. The model contains the longitudinal rigid-body states [u, w, θ q] and the longitudinal and lateral gimbal flap states [a_1 b_1] of rotor 1, together with their time derivatives. The two rotors behave identically to cyclic inputs, so retaining the dynamics of both in the longitudinal model would have led to redundancy in the form of unobservable/uncontrollable states.

H-infinity design involves first defining an interconnection structure (the one used here is shown in Fig. 31 below), then selecting a number of weights W_i, and finally using standard software routines to synthesise a controller that minimises the *H*-infinity norm ('gain') of the closed-loop transfer function, linking disturbances to penalty outputs as defined in the interconnection. The reader is referred to Ref. 23 for details of this approach. We present just an outline of the procedure as it was used.

The basic aims, with reference to the structure in Fig. 31 were to:

1. Reduce gain from η to [M_z, a] as much as possible. (i.e. reduce M_z and a for a given η).
2. Reduce gain from η to z_Δ to achieve desired gain margin at plant input.
3. Reduce energy in z_u due to all effects to limit the SLA's use of actuators.

In addition, the SLA law should have minimal impact on the pitch axis handling qualities of the aircraft. However, in order to reduce complexity, it was decided not to tackle this directly (although to do so would be quite feasible in principle). Instead, as for the case of the μ-synthesis controller, only the effect that the feedback law had on the handling qualities is shown.

Various weights W_i appear in the diagram. These trade-off the different objectives within the cost function. Very simple constant weights were used. The robustness weight W_Δ was set to 0·6. which amounts to specifying a nominal gain margin of [0·4-1·6]. The performance weight W_{perf} enables bending moment suppression to be traded off against gimbal flap. Typical bending moment variation was anticipated to be of the order ~1,000's ft-lbs, while flap excursions would be of the order 0·1 rad. M_z and a were weighted (multiplied) by $3{\cdot}26 \times 10^{-4}$ and 48·94 respectively in W_{perf}, these values being reciprocals of the anticipated variations. Finally, the control weight $W_u = 0{\cdot}1$ and the sensor noise weight $W_n = 0{\cdot}001$.

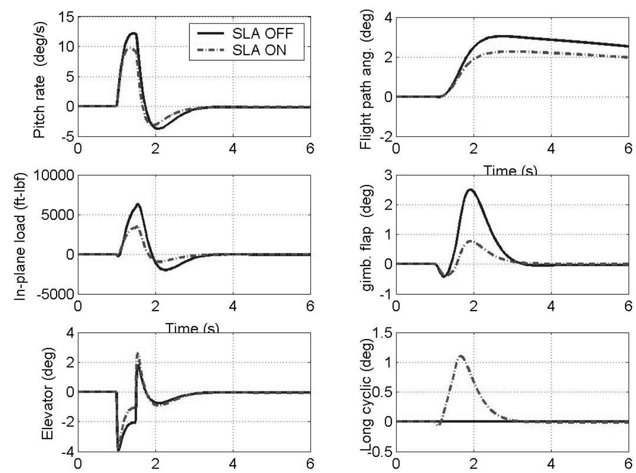

Figure 32. Response of EUROTILT to elevator at design condition; dual-objective design.

It is important to point out that the above parameters were actually developed and tuned for the FXV-15, prior to implementation in the EUROTILT configuration. Essentially, the results presented were obtained by substituting the EUROTILT linear model for that of the FXV-15 and re-synthesizing using the same weighting parameters. This led to a workable control law for EUROTILT, sufficient at least to demonstrate what might be possible on that aircraft, but the results should not be interpreted as being optimal in terms of EUROTILT performance.

5.11 Performance of four-state *H*-infinity SLA system

The process described above led to a stable, eight-state, two-input, two-output controller. It was possible to reduce further the number of states to four by model reduction without having any noticeable effect on the controller's behaviour. It was found that the SLA increased the damping of the short period mode. The response to an elevator pulse input at the design point with SAS engaged is shown in Fig. 32. Flight-path angle (γ) and pitch rate (q) responses with and without the SLA give some qualitative indication of the reduction in performance for the same pilot command, i. e. approximately 20%.

Also clear is the ability of the SLA to reduce M_z to about 50% of its open loop value, and gimbal longitudinal flap (here shown for rotor 2) to about 30% of its open loop value.

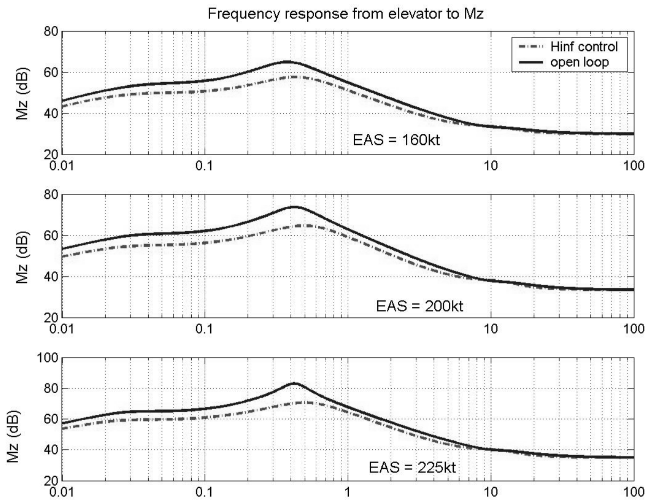

Figure 33. Bode plot showing M_z attenuation in EUROTILT.

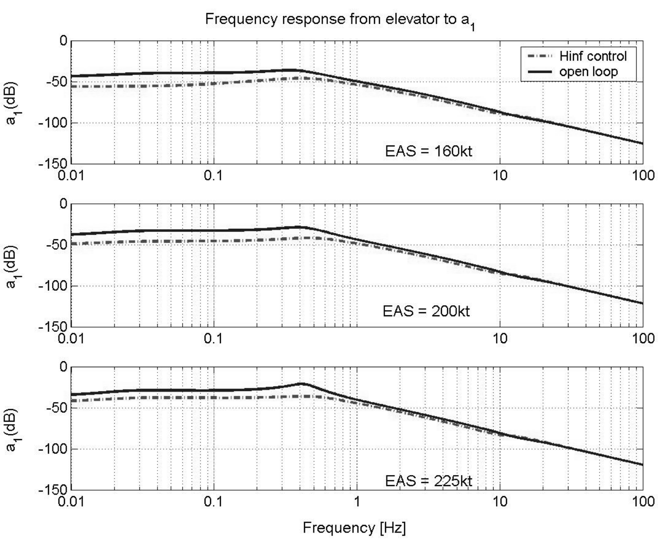

Figure 34. Bode plot showing gimbal flap attenuation in EUROTILT.

The gains from elevator-to-M_z and elevator-to-a were calculated using the reduced order controller and each of the three 17-state linearisations. The Bode magnitude plots are shown in Figs 33 and 34 for the off-design, 160kt flight condition. It can be seen that the control law provides 5-10dB reduction in M_z and 13-15dB reduction in gimbal flap over a wide band of frequencies.

The SLA performance achieved in this design required about 1deg of rotor cyclic and elevator. The sub-optimal performance is partly attributed to the re-use of the FXV-15 control law structure with the EUROTILT configuration; relatively lower gains being used on the larger machine. Nevertheless, the principles of the dual-objective control design concept have been demonstrated and the research continues with increased focus on EUROTILT in support of the final objectives of the RHILP project.

6.0 DISCUSSION

At the time of writing this paper, the first piloted simulation trials with EUROTILT with the combined Eurocopter SAS and CIRA/Liverpool SLA systems were being conducted on the Liverpool flight simulator with the full-envelope non-linear FLIGHTLAB simulation. The suppression and performance impact predicted by the off-line simulations have been broadly realised for longitudinal manoeuvres with similar amplitude and frequency content to the design cases. As the pilot explored the system behaviour in 'free flight', including larger amplitude manoeuvres, higher frequency tracking tasks and lateral manoeuvres, not surprisingly, aspects unexamined during the design process began to emerge. Amplification of loads was experienced during push-overs and also during lateral manoeuvres when sideslip angles were allowed to develop and a limit-cycle tendency followed on from cyclic saturation. These characteristics are under further investigation to establish if they arise through deficiencies in the control schemes themselves, or if they are systemic to the aircraft. These tentative findings reinforce the importance of piloted simulation in the overall assessment of a design concept as a relatively rapid method of exploring behaviour over a wide envelope.

Modelling for active control of SLA is a significant technical challenge met in the RHILP project by adopting the current, fairly universal, standard for real time, e.g. non-linear blade element rotors. The basic flight dynamic behaviour appears to be captured well by the modelling level adopted, but questions have been raised about the loads predictions. The test data available in the open literature, in-plane loads for example, is limited and certainly insufficient to provide a sound basis for confidence in this modelling level. There is a real need for experimental work in this area, to determine both in-plane and out-of-plane loads and flapping motions for correlation with theory. Aeroelastic effects also need to be quantified and the modelling requirements determined, particularly for 'soft' blade structures.

Two approaches to SLA system design have been presented, *viz*, μ-synthesis and *H*-infinity. The μ-synthesis approach used longitudinal cyclic as the controller output whereas the *H*-infinity method used elevator and cyclic for load reduction. In addition, the *H*-infinity method was formulated as a dual-objective problem, to suppress both the in-plane load and the gimbal longitudinal flap. Considerations of the trade-offs between performance and the HQs for the design and off-design conditions, in the presence of multiplicative output uncertainty, led to the selection of a SLA system that used gimbal angles and pitch rate as feedback measurements. For the case of the μ-synthesis design, a seven-state controller with 4 degs control authority provided acceptable performance with moderate degradation of handling qualities for the 200kt flight condition, as well as in the two specified off-design cases (160kt EAS at sea-level and 225kt EAS at 6,000m). For the same reference manoeuvre, the four-state *H*-infinity controller used approximately 1·2 deg of cyclic in addition to the elevator feed back. The performance was inferior (due to the reduced cyclic authority) compared to the μ-controller whereas the flapping remained within 1 deg compared to the 3 deg excursion for the μ-controller. The comparison should not be construed as favouring either technique, however, since the design work was conducted independently with different objectives. In addition the results from the *H*-infinity approach are recognised as being sub-optimal as they utilised the same structure as the design for the FXV-15. Generally, the power of both these modern multivariable techniques has been well demonstrated in this application, in terms of effectiveness, efficiency and robustness.

The specific example presented in the paper is one of perhaps six critical loads needing attention for tiltrotors. Published work on the V-22 has highlighted different approaches, both active and passive, to the suppression of other loads, although open publications on this work have not appeared for some time. The multi-objective aspects of SLA demand good physical insight into the potential conflicts to guide the control design process. The same is true for the design of an integrated SAS and SLA system. If the systems have a similar level of integrity, then there is an obvious benefit to performance to including both the load alleviation and HQs in the same integrated design scheme. These aspects are being considered in the continuing work.

The US experience to date suggests that structural load alleviation functions, along with flight envelope protection, are mandatory with a required reliability level of 10^{-9}, e.g. part of 'direct mode' in BA609[24]. This places stringent demands on SLA designs in terms of sensors, actuators, robustness and failure characteristics, aspects that have not been addressed in the current work. These issues are, however, being addressed in a companion Framework Programme 5 research project ACT-TILT, which is focussing on more detailed aspects of control functions required to achieve Level 1 handling performance and also on the effects of functional failures on handling qualities. The test configuration for this study is Agusta's tilt rotor/wing ERICA[25]. Outputs from this activity may well be published at a later date.

7.0 CONCLUSIONS AND RECOMMENDATIONS

The paper has presented results from an exploratory investigation into some of the issues associated with the active control of structural load alleviation for tilt rotor aircraft. The research acknowledges and builds on the work accomplished in the US over the last 15 years. The study has addressed modelling aspects, particularly the nature of the build up in dynamic loads during manoeuvres. Simulation models of both the Bell XV-15 and Eurocopter EUROTILT configurations have been developed within the FLIGHTLAB environment to support this work. Particular attention has been given in the paper to active control concepts for the suppression of rotor yoke, in-plane, bending loads during pitch manoeuvres with EUROTILT. A μ-synthesis approach to control law design has been outlined with the primary objective of reducing the transient loads using rotor controls and a secondary objective of maintaining performance and handling. A complementary synthesis, using *H*-infinity techniques, has shown how the dual-objectives of suppressing transient load and flapping during manoeuvres are feasible using both rotor cyclic and elevator controls. The main conclusions of the work to date are:

1. Blade element rotor modelling is considered adequate for predicting the basic flight dynamics of tilt rotors in aeroplane mode and also for predicting the overall trends in the blade root in-plane bending moments during manoeuvres. However, it is considered that more detailed aerodynamic/aeroelastic modelling is required to achieve the level of accuracy required for system design.
2. Linear output equations representing the envelope of the n/rev blade in-plane moments can be derived by transforming the individual blade loads into a multi-blade-coordinate system. Output equations for the in-plane load envelope can also be approximated by a linear function of gimbal tilt rate and aircraft pitch rate. Both methods were found to be useful in representing the moment envelope during pitch manoeuvres in the control design process.
3. Load and flight path quickness are appropriate parameters for quantifying the effect of SLA system on load suppression and handling qualities.
4. The use of longitudinal cyclic was found to be an effective way of reducing the in-plane load during pitch manoeuvres in aeroplane mode with small-moderate penalties on handling performance. In the case of EUROTILT, it was found that the in-plane load excursions for the reference manoeuvre at the design flight condition (200kt EAS, 3,000m) could be fully attenuated with 7 deg of longitudinal cyclic accompanied by a 20% degradation in HQs. However, longitudinal gimbal flap angles of similar magnitude as the applied cyclic were induced by the SLA system. The *H*-infinity method addressed this problem by formulating the dual-objective function to reduce both moments and flapping by utilising elevator feed back in addition to rotor cyclic. The *H*-infinity method was effective with the inevitably greater penalty on HQs due to the use of elevator feedback.
5. In the single-objective approach with a controller authority constraint of 4 deg, the load was suppressed to about 40% of its open loop value with a corresponding 10% reduction in flight path performance at the reference condition. A similarly small degradation in performance was exhibited at the off-design flight conditions investigated.

The continuing research in RHILP and the follow-on ACT-TILT project will be informed by the lessons learned to date and guided by the following recommendations.

1. In the longer term, experimental data is required to enhance confidence in the modelling of *n*/rev loads on prop-rotors in aeroplane and conversion modes. More comprehensive aerodynamic/aeroelastic models (e.g. higher fidelity FLIGHTLAB options) should be used in the short term to calibrate the current modelling level.
2. The techniques outlined should be applied to the assessment of the yoke load/flap suppression in other manoeuvres/flight case and the suppression of other critical loads.
3. Techniques for integrating the design of the core SAS and SLA functions should be explored.

ACKNOWLEDGEMENTS

The work reported in this paper was part sponsored by the European Commission as part of the Fifth Framework Programme. The members of the RHILP team involved with this activity are largely acknowledged in the authorship but recognition should also be given to German Roth of Eurocopter Deutschland who contributed to the development of our understanding of the critical loads relevant to tilt rotor aircraft manoeuvring. This paper was originally presented at the 59th Annual Forum of the American Helicopter Society in Phoenix, Arizona, May 2003.

REFERENCES

1. ROLLET, P. RHILP — A major step for European knowledge in tiltrotor aeromechanics and flight dynamics, 2001, Aeronautics Days 2001, Hamburg, Germany, January 28-31, 2001.
2. KING, D.W., DABUNDO, C. and KISOR, R.L. V-22 load limiting control law development, 1993, 49th Annual Forum of the American Helicopter Society, May 1993.
3. LANDIS *et al* Advanced flight control technology achievements at Boeing Helicopters, 1994, *Int J Control*, **59**.
4. MILLER, D.G., BLACK, T.M. and JOGLEKAR, M. Tiltrotor control law design for rotor loads alleviation using modern control techniques, 1991, American Control Conference, Evaston, IL, USA, June 1991, **3**, pp 2488-2495.
5. MILLER, D.G. and HAM, N.D. Active control of tiltrotor blade in-plane loads during maneuvers, 1988, 14th European Rotorcraft Forum, Milan, Italy, September 1988.
6. AGNIHOTRI, W., SCHUESSLER, R. and MARR. V-22 aerodynamic loads analysis and development of loads alleviation flight control system, 1989, 45th Annual Forum of the American Helicopter Society, May 1989.
7. MEYER, M. and PADFIELD, G.D. First steps in the development of handling qualities criteria for a civil tiltrotor, 2002, 58th American Helicopter Society Annual Forum, Montreal, June 2002.
8. DESOPPER, A. *et al* Study of the low speed characteristics of a tiltrotor, 2002, 28th European Rotorcraft Forum, Bristol, UK, September 2002.
9. RENAUD, J., HUBER, H. and VENN, G. The EUROFAR program; A European overview on advanced VTOL civil transportation system, 1991, 17th European Rotorcraft Forum, Berlin, Germany.

10. ROLLET, P. and THIBAUDAT, C. EUROFAR simulation trials on EPOPEE simulator, 1992, 18th European Rotorcraft Forum, Avignon, France, September 1992.
11. PADFIELD, G.D. and WHITE, M.D. Flight simulation in academia; HELIFLIGHT in its first year of operation, 2001, The Challenge of Realistic Rotorcraft Simulation, RAeS Conference, London, November 2001. *Aeronaut J,* **107**, (1075), September 2003, pp 529-538.
12. HARENDRA, P.B. *et al* A mathematical model for real time flight simulation of the Bell Model 301 tiltrotor research aircraft, 1973, Bell Helicopter Company Report No 301-099-001, April 1973.
13. SCHILLINGS, J.J., ROBERTS, B.R., WOOD, T.L. and WERNICKE, K.G. Maneuver performance comparison between the XV-15 and an advanced tiltrotor design, *J American Helicopter Soc*, May 1990.
14. MAISEL, M. NASA/ARMY Tiltrotor research aircraft familiarization document, 1975, NASA TM X-62, 407, January 1975.
15. PETERS, D.A. and HE, C.J. Finite state induced flow models Part II, Three-dimensional rotor disc, *J Aircr* , **32**, (2), pp 323-333.
16. PADFIELD, G.D. *Helicopter Flight Dynamics*, 1996, Blackwell Science, Oxford.
17. GOLDSTEIN, K. and DOOLEY, L. V-22 control law development, 1986, 42nd Annual Forum of the American Helicopter Society, Washington DC, USA, June 1986, pp 673-684.
18. PACKARD, A. and DOYLE, J.C. The complex structured singular value, *Automatica*, 1993, **29**, (1), pp 71-109.
19. ZHOU, K., DOYLE, J.C. and GLOVER, K. *Robust and Optimal Control*, 1996, Prentice-Hall.
20. PAVEL, M. and PADFIELD, G.D. Defining consistent ADS-33 metrics for agility enhancement and structural loads alleviation, 2002, 58th American Helicopter Society Forum, Montreal, June 2002
21. STEVENS, B.L. and LEWIS, F.L. *Aircraft Control and Simulation*, 1992, John Wiley and Sons, Chichester.
22. BALAS, G.J., DOYLE, J.C., GLOVER, K., PACKARD, A. and SMITH, R. *μ-Analysis and Synthesis Toolbox*, 1998, The Mathworks.
23. SKOGESTAD, S and POSTLETHWAITE, I. *Multivariable Feedback Control*, 1996, John Wiley and Sons, Chichester.
24. GAFFEY, T.M. BA609 Tiltrotor regulatory requirements, 2000, European Helicopter Association Symposium, The Hague, The Netherlands, September 2000.
25. NANNONI, F., GIANCAMILLI, G. and CICALE, M. ERICA: The European advanced tiltrotor, 2001, 27th European Rotorcraft Forum, Moscow, Russia, September 2001.

https://doi.org/10.1017/S0001924000000087 Published online by Cambridge University Press